Transoceanic infragravity waves impacting Antarctic ice shelves

Peter D. Bromirski,[1] Olga V. Sergienko,[2] and Douglas R. MacAyeal[3]

Received 23 October 2009; revised 24 November 2009; accepted 14 December 2009; published 29 January 2010.

[1] Long-period oceanic infragravity (IG) waves (*ca.* [250, 50] s period) are generated along continental coastlines by nonlinear wave interactions of storm-forced shoreward propagating swell. Seismic observations on the Ross Ice Shelf show that free IG waves generated along the Pacific coast of North America propagate transoceanically to Antarctica, where they induce a much higher amplitude shelf response than ocean swell (*ca.* [30, 12] s period). Additionally, unlike ocean swell, IG waves are not significantly damped by sea ice, and thus impact the ice shelf throughout the year. The response of the Ross Ice Shelf to IG-wave induced flexural stresses is more than 60 dB greater than concurrent ground motions measured at nearby Scott Base. This strong coupling suggests that IG-wave forcing may produce ice-shelf fractures that enable abrupt disintegration of ice shelves that are also affected by strong surface melting. Bolstering this hypothesis, each of the 2008 breakup events of the Wilkins Ice Shelf coincides with wave-model-estimated arrival of IG-wave energy from the Patagonian coast. **Citation:** Bromirski, P. D., O. V. Sergienko, and D. R. MacAyeal (2010), Transoceanic infragravity waves impacting Antarctic ice shelves, *Geophys. Res. Lett.*, *37*, L02502, doi:10.1029/2009GL041488.

1. Introduction

[2] Despite early observations of the prominent influence of sea swell on iceberg, ice-shelf and ice-tongue flexure [*Holdsworth and Glynn*, 1978; *Williams and Robinson,* 1979; *Wadhams et al.,* 1983], there have been few systematic field measurements or theoretical studies of the effects of gravity waves on ice shelves until very recently [*Sergienko et al.,* 2008; *MacAyeal et al.,* 2009]. Ocean gravity waves can potentially affect ice shelf stability in several ways: by opening crevasses, reducing ice integrity through fracturing, and by initiating a collapse event. A recent field measurement advance stems from the deployment of a broadband seismometer on the Ross Ice Shelf during 2004–2006 at a site called 'Nascent Iceberg' (Figure 1b, station RIS2). Initial study of these data [*Okal and MacAyeal,* 2006; *MacAyeal et al.,* 2006; *Cathles et al.,* 2009] showed that the ice shelf is continually flexed by ocean swell (<30 s period) originating primarily under far-field Pacific storms. Analyses of these seismometer data presented here show that even more significant mechanical impacts on the Ross Ice Shelf result from another type of surface gravity wave—infragravity (IG) waves with periods from about 250 to 50 s (0.004 to 0.02 Hz), primarily generated by nonlinear-wave interactions along coastlines [*Longuet-Higgins and Stewart,* 1962; *Herbers et al.,* 1994, 1995a, 1995b].

2. IG Wave and Swell Observations on the Ross Ice Shelf: Comparative Amplitudes and Source Regions

[3] Some of the IG wave energy generated along coastlines leaks off continental shelves and becomes free waves. The free IG waves propagate dispersively in deep water, causing a large time lag between lower and higher frequency waves when travelling from the West Coast to Antarctica. When gravity waves propagate from deep to shallow water, shoaling causes their amplitude to increase. Because IG wave wavelengths are much longer than swell, IG amplitudes will be enhanced relatively more than swell amplitudes by shoaling at the front of the Ross Ice Shelf (water depth 600 m). Refraction of IG waves on the Antarctic continental shelf also likely affects IG wave amplitudes at the ice front, focusing and defocusing depending on local bathymetry.

[4] IG waves impacting the West Antarctica coast cause flexure of the Ross Ice Shelf. The ice shelf response to IG wave forcing can be seen in difference spectrograms (where the mean spectrum is removed from the raw spectra) from on-ice seismic station RIS2 during the 2005/6 austral summer (December through April, Figure 1). Swell and IG wave arrivals are identified in the spectrograms by vertical and upward slanting positive-anomaly bands. Because lower-frequency waves travel faster (i.e., according to the deep-water gravity wave dispersion relation), the slope of each slanting band gives an estimate of the distance to the generation region, with shallower slopes indicating longer propagation paths. Vertical bands denote local-to-regional wave events. Most of the very long period swell (from about 30 s to 18 s, 0.03 to 0.07 Hz) and IG-wave energy (at frequencies <0.02 Hz) reaching the Ross Ice Shelf during the austral summer is strongly dispersed (Figures 1a and 1c), indicating a North Pacific source location.

[5] The Ross Ice Shelf is impacted by multiple gravity wave arrivals throughout the austral summer, with characteristic high-amplitude events described below. Counter-clockwise cyclonic winds along the trailing edge of the mid-Pacific storms force swell directly toward Antarctica, which occurs for waves from a storm on February 4, 2005 (track c in Figure 1b). Waves from another storm were concurrently impinging the West Coast of North America. The right-front quadrant winds of the mid-Pacific storm and the storm's propagation direction additionally force waves toward the Gulf of Alaska, reaching the coast on February 6

[1]Scripps Institution of Oceanography, University of California, San Diego, La Jolla, California, USA.
[2]AOS Program, Princeton University, Princeton, New Jersey, USA.
[3]Department of the Geophysical Sciences, University of Chicago, Chicago, Illinois, USA.

0094-8276/10/2009GL041488$05.00

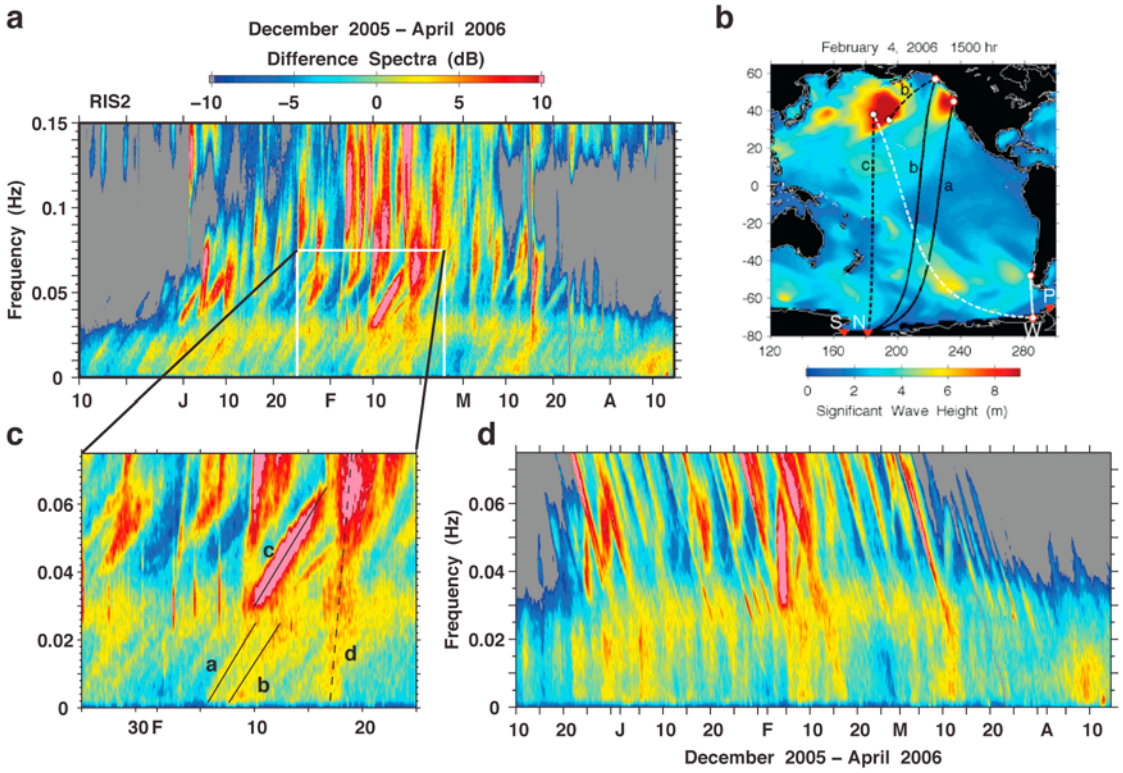

Figure 1. Ross Ice Shelf (RIS2) seismometer data. (a) Difference spectrogram of vertical component data, collected near the front of the Ross Ice Shelf (RIS2) at Nascent Iceberg, labeled 'N' in Figure 1b, obtained by subtracting the mean spectrum over the entire period. As the mean spectrum has a large amplitude range (see Figure 2b), relative amplitude comparisons are only valid across relatively narrow frequency bands. Near vertical bands indicate that the waves were generated by nearby storms, while strongly slanted bands indicate dispersed arrivals from storms in the North Pacific. (b) WAVEWATCH III (WW3) (H. L. Tolman, Manual and wave user system documentation of WAVEWATCH-III version 2.22, U.S. Department of Commerce, 2005; hindcast files available from http://polar.ncep.noaa.gov) model wave height, H_s, for the mid-Pacific storm event causing the dominant swell signal at RIS2 on Feb. 10–14; a concurrent wave event reached the West Coast. Propagation trajectories (great circle paths) for both direct swell (dashed) and coastally generated IG waves (solid). The seismic data collected at Scott Base and Palmer Station, 'S'and 'P' provide land-based seismic observations used in comparison with data collected at N. The Wilkins Ice Shelf, 'W' is likely subjected to strong IG-wave energy generated along the Patagonia coast, as well as potentially from North Pacific swell (white tracks). (c) Detail of the box in Figure 1a showing that the forward modeled dispersion trends for the tracks in Figure 1b match the underlying ice-shelf signals, with the slight differences in slope resulting from the different path lengths. Regional storm event swell signal above 0.05 Hz and associated IG energy at frequencies <0.035 Hz (dashed trend d). Transient vertical striations near 0.03 Hz on, e.g., Feb. 2, 4, and 6 are earthquake signals. (d) Difference spectrum corrected for gravity wave dispersion and travel time from the West Coast location to the Ross Ice Shelf for track a.

(track b, also see Text S1, section S1).[1] Swell from each of these storms is subsequently transformed to IG waves when their eastward propagating waves reach the West Coast. A portion of the coastal IG wave energy leaks off the continental shelf and follows great circle paths (tracks a and b, respectively) to the Ross Ice Shelf (N, Figure 1b). Forward modeling of swell and IG wave propagation from assumed source locations (solid dots, Figure 1b) to the Nascent seismometer using the gravity wave dispersion relation gives the associated dispersion curves in Figure 1c (black lines), in good agreement with the underlying spectral energy trends.

[6] In addition to North Pacific IG wave arrivals, the circum-Antarctic ocean is also a source of swell energy that reaches the Ross Ice Shelf. Bound waves associated with swell groups force locally generated IG-wave band energy when the swell groups propagate into shallow continental-shelf water [*Longuet-Higgins and Stewart,* 1962; *Herbers et al.,* 1994, 1995a, 1995b]. Locally generated IG-wave energy is identified in the data on February 17, 2005, evidenced by the extension of energy along the steep dispersion trend for that event to lower IG wave frequencies (Figure 1c, dashed trend d). Locally forced IG waves associated with strong regional storms apparently also occur on January 4, February 9, and March 15, indicating that swell-group induced local IG-wave excitation is not rare and may also affect ice shelf integrity over time.

[7] IG waves have much longer wavelengths than swell (on the order of 20 km vs. less than 1 km in the 600 m water depth at the front of the Ross Ice shelf) and span a much larger bandwidth, causing the mechanical effect on the ice

[1]Auxiliary materials are available in the HTML. doi:10.1029/2009GL041488.

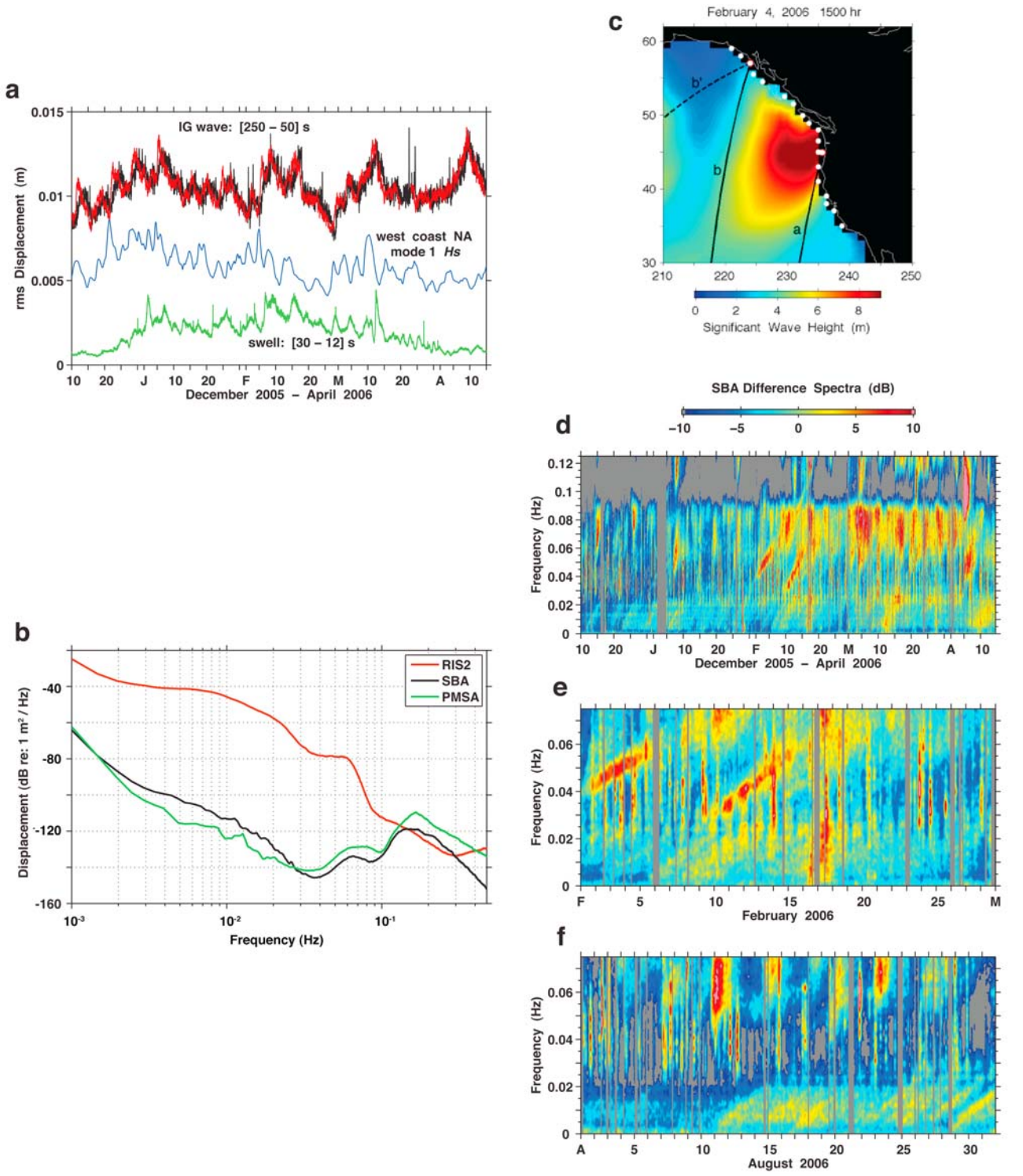

Figure 2. IG-wave induced ice motion vs. ground motion at land stations. (a) Vertical root-mean-square (rms) displacement amplitudes spanning the [250, 50] s period IG-wave band (black, see Figure 1a) and dispersion-travel time corrected spectra (red, see Figure 1d), and swell band (green, [30, 12] s period) recorded by the RIS2 seismometer (N in Figure 1b). Transient spikes are earthquake signals. (b) Mean vertical component displacement spectral levels over the Nov. 2005–April 2006 period near the calving front of the Ross Ice Shelf (RIS2, red) and at Antarctic land-based seismic stations at Scott Base (SBA, black; S in Figure 1b) and Palmer Station (PMSA, green; P in Figure 1b). (c) Location of WW3 wave-model grid nodes (white dots; overlaid on H_s data from Figure 1b) used to determine the mode 1 principal component time series (blue curve in Figure 2a). (d) Difference spectrum, formed by subtracting the mean spectrum for the time period shown, from on-land seismic station at Scott Base (S in Figure 1b); compare with Figure 1a. (e) and (f) Difference spectra for Scott Base, formed by subtracting the mean spectrum for January 2006, during February and August, 2006.

shelf to be larger for low-frequency IG waves than for higher frequency swell. This expectation is confirmed by comparison of root mean square (rms) displacement amplitudes (Figure 2a): the magnitude of IG-wave band motion is in the centimeter range (rms), whereas that of the swell band is in the millimeter range. During the austral summer, when sea ice is at a minimum, rms amplitudes of IG waves are about a factor of 3 greater than swell, but this factor increases to about 15 when sea ice is present. This shows that the impact of the much longer period IG waves on ice shelves is not greatly affected by sea ice, but swell is significantly damped. The year-round flexing of the Ross Ice Shelf by IG waves underscores their potential long-term impact on ice shelf integrity, unlike tsunamis that are much less frequent and generally of shorter duration.

[8] An additional demonstration of the greater impact of IG waves on the Ross Ice Shelf is provided by comparison of spectral levels on the Ross Ice Shelf (RIS2) with those at Antarctic land-based seismic stations (Figure 2b). Mean amplitudes recorded by the land-based seismic stations at Scott Base and Palmer Station (SBA and PMSA, 'S' and 'P' in Figure 1b, respectively) vary within a relatively narrow amplitude range across the swell (0.03 to 0.085 Hz) and IG-wave (0.004 to 0.02 Hz) frequency bands, with amplitudes similar to those observed globally. The difference between SBA and RIS2, however, illustrates the great sensitivity of the ice-shelf response to IG-wave forcing. RIS2 levels are more than 3 orders of magnitude greater than those of SBA and PMSA at 100-s period (0.01 Hz).

[9] IG-wave variability along the West Coast of North America that forces the Earth's 'hum' during winter months is well correlated with wave model significant wave height (H_s, the average of the highest 1/3 of the waves) north of Cape Mendocino [*Bromirski and Gerstoft,* 2009]. This relationship is used to confirm the West Coast-Ross Ice Shelf connection. The leading, "mode 1" principal component of wave model H_s along the West Coast (Figure 2c) was correlated with a representative IG-wave time series derived from the Ross Ice Shelf data (Figure 2a). Because IG waves in the generation region are not dispersed, the RIS2 spectral data must first be corrected for frequency-dependent dispersion to appropriately test their similarity. Although multiple IG-wave generation locations along the West Coast clearly occur (Figure 1a; see *Bromirski and Gerstoft*, 2009), correcting for dispersion shows that the different IG-wave travel path lengths are not problematic, evidenced by the near vertical bands for IG-wave band energy (Figure 1d) that are consistent with an approximately common source region. The correlation coefficient (R) of the dispersion-corrected IG-wave rms time series in the [250, 50] s period band (Figure 2a, red) with mode 1 wave model H_s (Figure 2a, blue) over the Dec. 20, 2005 to March 15, 2006 time period is R = 0.79. This good correlation gives further confirmation that the dominant IG-wave source region is the Pacific coast of North America. Additionally, correlation of the uncorrected RIS2 rms IG-wave time series (Figure 2a, black) with the SBA rms vertical displacement amplitude over the same [250, 50] s period band from Dec. 20, 2005–March 15, 2006 gives R = 0.75, indicating SBA seismic data can be used to characterize the Ross Ice Shelf response to IG wave energy. Dispersed IG wave arrivals observed at SBA during August have similar amplitudes to those during February when sea ice is at a minimum (compare Figures 2e–2f, 0.002–0.02 Hz). This confirms RIS2 observations (Figure 2a) that sea ice has minimal effect on free IG-wave propagation near the Antarctic coast, and that transoceanic IG waves induce mechanical stresses on the Ross Ice Shelf throughout the year.

[10] That dispersed IG-wave arrivals are observed at SBA (Figure 2d, at frequencies <0.03 Hz) suggests that free IG waves impacting distant coasts may contribute to the Earth's 'hum' [*Rhie and Romanowicz,* 2006]. However, these dispersed IG arrivals could not be identified at other Antarctica seismic stations (see Text S2), suggesting that (1) these signals are not hum Rayleigh waves, (2) the hum signal strength was too low to be observed at more distant individual stations, or (3) that these signals result from conversion of IG-wave induced perturbation stresses propagating through the ice shelf to seismic elastic body waves inland from the grounding zone. If this last possibility applies, these phases could be useful for detecting changes in ice shelf integrity.

[11] Note that the North Pacific dispersed swell and IG wave induced signals are observed at their respective gravity wave frequencies, but the typically much higher amplitude associated double-frequency signals [*Longuet-Higgins*, 1950] are not observed (Figures 1a, 1c, and 2d–2f). Narrow-band dispersed austral swell arrivals along the Oregon coast also produced no double-frequency signals [*Bromirski and Duennebier*, 2002]. These observations indicate either an absence of opposing wave energy for these arrivals due to dissipation from sea floor interaction, or that the area of wave-wave interaction is small. Hum Raleigh waves are generated by the wave-wave mechanism [*Webb*, 2008]. To produce hum that has the pattern of the low-amplitude dispersed IG wave-induced signals at SBA requires their transformation to lower frequencies. However, wave steepness of the incident IG wave arrivals is likely too low for significant transformation to lower frequencies to occur. Additionally, damping by sea ice during the austral winter would also likely reduce any nonlinearity of incident IG waves, making the necessary wave-wave interactions less likely. Consequently, because of these factors and because similar amplitude dispersed IG wave-induced signals are observed at SBA during both the austral winter and the austral summer (Figures 2f and 2e), these signals are most likely not hum.

3. Ice-Shelf Flexure Modeling

[12] To estimate effects of IG waves on the ice-shelf stress regime we have developed a 2-dimensional, vertical cross-section finite-element model with idealized, constant-thickness geometry (O. V. Sergienko, manuscript in preparation, 2009). The ocean is treated as an incompressible, inviscid fluid where motion is described by a velocity potential. Flexure of the ice shelf is governed by the momentum equation with Hook's law as a constitutive relationship with parameters selected for ice. Coupling of wave energy to the ice-shelf is simulated by representing the wave-induced normal stresses at the water/ice interfaces.

[13] Model simulations were performed for two idealized geometries to estimate the flexural stresses produced at the

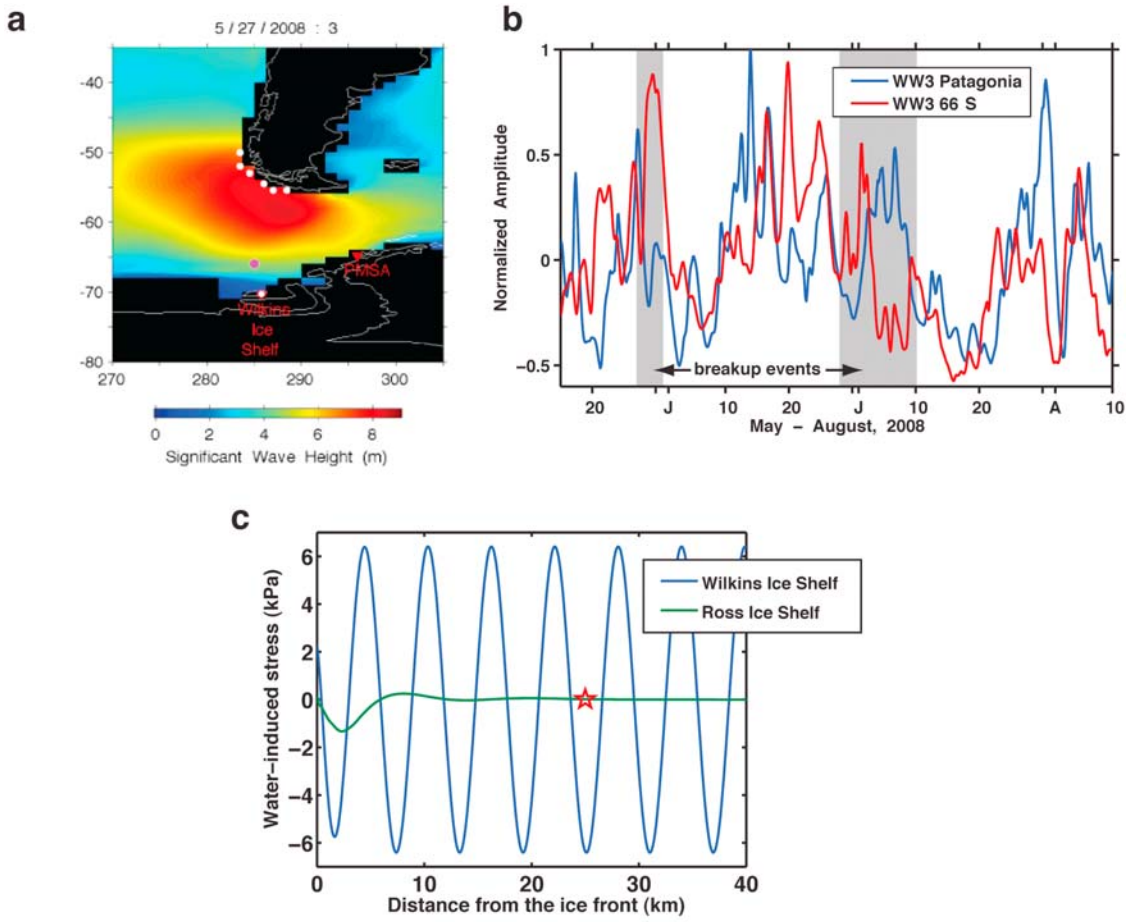

Figure 3. IG-wave generation along Patagonia coast possibly triggering the Wilkins Ice Shelf breakup. (a) Wave model H_s distribution just prior to the end-of-May 2008 initiation of the Wilkins Ice Shelf collapse. (b) Normalized time series: The mode 1 principal component variability at wave model grid nodes along the Patagonia coast (WW3 *Patagonia*, blue; at white dots in Figure 3a), and model H_s near the Wilkins Ice Shelf (WW3 66S, red; magenta dot in Figure 3a denotes the center location of a 5-grid node average). Time periods associated with Wilkins-Ice-Shelf breakup events (shaded gray) correspond with periods of heightened wave amplitude estimated by the wave model data. (c) Calculated stresses at the ice-shelf surface (where crevasses initiate) induced by a 30 cm amplitude, 175 s period IG wave impacting uniformly thick floating ice slabs that idealize the regional ice-front conditions of the Wilkins Ice Shelf (100 m ice thickness, 300 m water depth) and the Ross Ice Shelf (300 m ice thickness, 600 m water depth). A star denotes the equivalent location of the RIS2 seismometer relative to the ice front of the idealized ice shelf. The amplitude of the IG wave was chosen so modeled displacements matched the measured RIS2 surface displacement at this distance from the front (Figure 2a).

surface of two idealized ice shelves (Figure 3c). These stresses are deviations from the steady-state flexural stresses caused by the hydrostatic pressure-induced bending moment at the ice-shelf front. The magnitude of the wave induced stresses is ~5% of the steady-state values. The wave-induced stresses have a complex spatial distribution through the ice-shelf thickness with maximum amplitude achieved at both surfaces – top and bottom – locations where crevasses develop.

4. Discussion: IG-Waves as Ice-Shelf Collapse Triggers?

[14] The mechanisms producing explosive ice-shelf collapse events of the Antarctic (e.g., Larsen B in 2002, Wilkins in 2008) remain only partially identified, because the time scale of collapse is simply too short (hours to days) to allow sufficient satellite passes to observe the process in flagrante (http://nsidx.org/news/press/Larsen_b/2002.html; and http://nsidc.org/news/press/20080325_Wilkins.html). Leading theories suggest that abundant free surface water (e.g., in ponds that fill surface depressions and crevasses) fills pre-existing crevasses, constituting the principle enabling condition for collapse [*Scambos et al.,* 2000, 2009]. The mechanisms that produce the pre-existing crevasses and that provide the proximal trigger for the collapse remain unknown. We propose here that southbound travelling IG waves produced by storms in the far field (i.e., located remote from Antarctica) may be a key mechanical agent that contributes to the production and/or expansion of the pre-existing crevasse fields on ice shelves, and that the IG waves thus provide the trigger necessary to initiate the collapse process.

[15] Support for this hypothesis is provided by four considerations. First, these observations demonstrated that, because of sea ice damping, sea-swell energy is less likely than IG-wave energy to couple to crevasse-producing/expanding flexure stresses in the ice shelf. Second, the available satellite observations of the March 2002 Larsen B event and the February 29, 2008, Wilkins Ice Shelf event show that they started in calm weather, suggesting that the trigger was non local, e.g., an incoming IG-wave group. Third, the austral-winter collapse episodes of the Wilkins Ice Shelf (i.e., in May and June/July of 2008) rule out the possibility that a slow increase of surface meltwater-load provided the immediate trigger. Fourth, there is indirect evidence that IG-wave radiation to Antarctica from source regions along the South American coast may have played an integral role in the May–July, 2008 collapse of the Wilkins Ice Shelf ('W' in Figure 1b, propagation path solid white).

[16] Wave model H_s variability along the southern Patagonia coast (Figure 3a, Animation S1) gives an estimate of IG-wave generation [*Bromirski and Gerstoft,* 2009] in a source region that would subsequently impact the Wilkins Ice Shelf. IG-wave propagation time from Patagonia to Wilkins is <12 hr; thus, correspondence of IG-wave amplitude peaks associated with mode-1 H_s variability along the Patagonian coast (Figure 3b) with the times of major breakup episodes is a compelling reason to consider IG-wave excitation as a factor in the ice-shelf breakup process. IG waves forced by local swell groups (Figure 3b, red) could also have contributed to the breakups. Although these associations of wave model H_s with the Wilkins breakup are not conclusive, it is clear that further observations are justified to better characterize the amplitude, temporal variability, and potential source areas of IG waves, in conjunction with glaciological modeling of ice-shelf wave interaction, to understand their impact on ice-shelf integrity.

[17] **Acknowledgments.** The California Department of Boating and Waterways provided funding support for Bromirski. Sergienko is supported by NSF grant OPP-0838811 and by a fellowship from the AOS of Princeton University. We thank Ron Flick, Myrl Hendershott, and Bob Guza for helpful IG wave discussions and Ralph Stephen and Barbara Romanowicz for seismology related comments. The RIS2 data were collected under NSF grant OPP-0229546 and were downloaded from the IRIS DMC archives. We thank the referees for their helpful comments.

References

Bromirski, P. D., and F. K. Duennebier (2002), The near-coastal microseism spectrum: Spatial and temporal wave climate relationships, *J. Geophys. Res.*, *107*(B8), 2166, doi:10.1029/2001JB000265.

Bromirski, P. D., and P. Gerstoft (2009), Dominant source regions of Earth's ''hum,'' *Geophys. Res. Lett.*, *36*, L13303, doi:10.1029/2009GL038903.

Cathles, L. M., IV, E. A. Okal, and D. R. MacAyeal (2009), Seismic observations of sea swell on the floating Ross Ice Shelf, Antarctica, *J. Geophys. Res.*, *114*, F02015, doi:10.1029/2007JF000934.

Herbers, T. H. C., S. Elgar, and R. T. Guza (1994), Infragravity-frequency (0.005–0.05 Hz) motions on the shelf. Part I: Forced waves, *J. Phys. Oceanogr.*, *24*(5), 917–927, doi:10.1175/1520-0485(1994)024<0917:IFHMOT>2.0.CO;2.

Herbers, T. H. C., S. Elgar, and R. T. Guza (1995a), Generation and propagation of infragravity waves, *J. Geophys. Res.*, *100*(C12), 24,863–24,872, doi:10.1029/95JC02680.

Herbers, T. H. C., S. Elgar, R. T. Guza, and W. C. O'Reilly (1995b), Infragravity-frequency (0.005–0.05 Hz) motions on the shelf. Part II: Free waves, *J. Phys. Oceanogr.*, *25*(6), 1063–1079, doi:10.1175/1520-0485(1995)025<1063:IFHMOT>2.0.CO;2.

Holdsworth, G., and J. Glynn (1978), Iceberg calving from floating glaciers by a vibrating mechanism, *Nature*, *274*(5670), 464–466, doi:10.1038/274464a0.

Longuet-Higgins, M. (1950), A theory of the origin of microseisms, *Philos. Trans. R. Soc. London, Ser. A*, *243*, 1–36, doi:10.1098/rsta.1950.0012.

Longuet-Higgins, M., and R. W. Stewart (1962), Radiation stress and mass transport in gravity waves, with application to ''surf beats,'' *J. Fluid Mech.*, *13*(4), 481–504, doi:10.1017/S0022112062000877.

MacAyeal, D. R., et al. (2006), Transoceanic wave propagation links iceberg calving margins of Antarctica with storms in tropics and Northern Hemisphere, *Geophys. Res. Lett.*, *33*(17), L17502, doi:10.1029/2006GL027235.

MacAyeal, D. R., E. A. Okal, R. C. Aster, and J. N. Bassis (2009), Seismic observations of glaciogenic ocean waves (micro-tsunamis) on icebergs and ice shelves, *J. Glaciol.*, *55*(190), 193–206, doi:10.3189/002214309788608679.

Okal, E. A., and D. R. MacAyeal (2006), Seismic recording on drifting icebergs: Catching seismic waves, tsunamis and storms from Sumatra and elsewhere, *Seismol. Res. Lett.*, *77*(6), 659–671, doi:10.1785/gssrl.77.6.659.

Rhie, J., and B. Romanowicz (2006), A study of the relation between ocean storms and the Earth's hum, *Geochem. Geophys. Geosyst.*, *7*, Q10004, doi:10.1029/2006GC001274.

Scambos, T., C. Hulbe, M. Fahnestock, and J. Bohlander (2000), The link between climate warming and ice shelf break-ups in the Antarctic peninsula, *J. Glaciol.*, *46*(154), 516–530, doi:10.3189/172756500781833043.

Scambos, T., H. A. Fricker, C.-C. Liu, J. Bohlander, J. Fastook, A. Sargent, R. Massom, and A.-M. Wu (2009), Ice shelf disintegration by plate bending and hydro-fracture: Satellite observations and model results of the 2008 Wilkins ice shelf break-ups, *Earth Planet. Sci. Lett.*, *280*(1–4), 51–60, doi:10.1016/j.epsl.2008.12.027.

Sergienko, O. V., D. R. MacAyeal and C. L. Hulbe (2008), Flexural-gravity wave phenomena on ice shelves, *Eos Trans. AGU*, *89*(53), Fall Meet. Suppl., Abstract C31D-0536.

Wadhams, P., M. Kristensen, and O. Orheim (1983), The response of Antarctic icebergs to ocean waves, *J. Geophys. Res.*, *88*(C10), 6053–6065, doi:10.1029/JC088iC10p06053.

Webb, S. C. (2008), The Earth's hum: The excitation of Earth's normal modes by ocean waves, *Geophys. J. Int.*, *174*(2), 542–566, doi:10.1111/j.1365-246X.2008.03801.x.

Williams, R. T., and E. S. Robinson (1979), Ocean tide and waves beneath the Ross Ice Shelf, *Antarct. Sci.*, *203*(4379), 443–445.

P. D. Bromirski, Scripps Institution of Oceanography, University of California, San Diego, La Jolla, CA 92093-0209, USA. (pbromirski@ucsd.edu)

D. R. MacAyeal, Department of the Geophysical Sciences, University of Chicago, Chicago, IL 60637, USA.

O. V. Sergienko, AOS Program, Princeton University, Princeton, NJ 08540, USA.